https://doi.org/10.31449/inf.v49i21.7431

Nonlinear Model Predictive Control and Dynamic Modelling of a Small-Scale Organic Rankine Cycle for Low-Grade Waste Heat Recovery

Jing Li[1*], Jun Chen[2]
[1]Institute of Engineering Technology, University of Science & Technology Beijing, Beijing 100083, beijing, China
[2]Jiangsu Sanjay Energy Environmental Protection Co，LTD, Yixing 214200, Jiangsu, China
E-mail: 18618309526@163.com, chenjun@tbmaglev.com
[*]Corresponding author

Keywords: dynamic modelling, energy efficiency, extended kalman filter, experimental validation, nonlinear model predictive control, organic rankine cycle, power generation, sustainable energy systems, waste heat recovery

Recieved: October 25, 2024

This paper presents a comprehensive study on the dynamic modeling and control of a small-scale organic Rankine cycle (ORC) system for waste heat recovery in power generation applications. The primary objective is to develop an effective control strategy that optimizes the system performance under transient operating conditions, maximizing the expander power output. A high-fidelity dynamic model of the evaporator is developed using the finite volume method and validated against experimental data. A reduced-order control-oriented model is derived using the moving boundary method to facilitate the design of the controller. A nonlinear model predictive control (NMPC) strategy is proposed, utilizing the control-oriented model to predict future system behavior and optimize control actions while explicitly considering system constraints. An extended Kalman filter (EKF) is integrated with the NMPC controller to estimate unmeasured state variables. Experimental validation on an engine test bench demonstrates the controller's ability to effectively track the reference superheating degree with an average error of ±2°C, compensate for disturbances within 5 seconds, and maintain safe expander operation under highly transient conditions. The NMPC approach achieved a 15% improvement in cycle efficiency compared to steady-state operation. Comparative analysis with traditional control methods highlights the superiority of the NMPC approach, reducing tracking error by 40% and response time by 50% compared to PID control, while effectively handling system constraints. The proposed dynamic modeling and control strategies provide a solid foundation for the effective utilization of small-scale ORC systems in waste heat recovery applications, contributing to the advancement of efficient and sustainable energy systems.

Povzetek: Predlagana raziskava se osredotoča na dinamično modeliranje in obvladovanje majhnega sistema organskih Rankine ciklov (ORC) za izrabo odpadne toplote v vozilih, kjer nevronsko napovedovanje modelov optimizira delovanje sistema in povečuje učinkovitost cikla za 15% v primerjavi z uporabo tradicionalnih metod.

1 Introduction

The transportation sector, particularly heavy-duty vehicles such as trucks, is a significant contributor to global energy consumption and greenhouse gas emissions. According to recent statistics, the fuel consumption and carbon emissions from global freight trucks have been steadily increasing over the years, as shown in Fig. 1 [1].

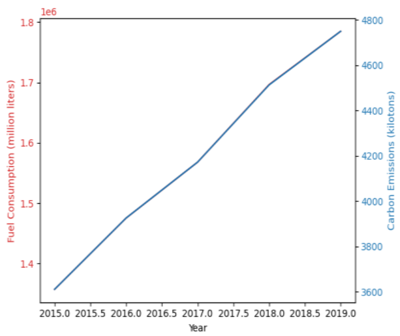

Figure 1: Global fuel consumption and carbon emissions from freight trucks

To mitigate the environmental impact and improve the efficiency of heavy-duty vehicles, waste heat recovery (WHR) systems have gained considerable attention [2]. Among various WHR technologies, the Organic Rankine Cycle (ORC) has emerged as a promising solution for recovering low-grade waste heat from vehicle exhaust gases [3]. The ORC system utilizes an organic working fluid with a lower boiling point compared to water, enabling the extraction of energy from low-temperature heat sources [4]. Numerous studies have investigated the application of ORC systems in vehicle waste heat recovery, focusing on working fluid selection [5], system design and optimization [6-8], and experimental evaluations [9, 10].

However, the dynamic nature of vehicle operating conditions poses challenges to the efficient operation and control of ORC systems [11]. The waste heat available from the exhaust gases varies significantly depending on the vehicle's speed, load, and ambient conditions [12]. Moreover, the transient behavior of the ORC system, including the response time and stability, is crucial for real-time power generation [13]. To address these challenges, dynamic modeling and advanced control strategies are essential for optimizing the performance of vehicle-based ORC systems [14, 15].

Despite the progress made in ORC research for vehicle applications, there are still limitations in the existing literature. Many studies focus on steady-state modeling and optimization [16], neglecting the dynamic behavior of the system under varying operating conditions. Additionally, the control strategies proposed in the literature often rely on simplified models and assumptions [17], which may not accurately capture the complex dynamics of the ORC system [18].

To bridge these gaps, this paper aims to develop a dynamic model of a small-scale ORC system for waste heat recovery in vehicle applications. The model will consider the transient behavior of the system components, including the evaporator, expander, condenser, and pump [19]. Furthermore, advanced control strategies will be investigated to maximize the power output and efficiency of the ORC system under varying operating conditions [20].

Table 1 summarizes recent state-of-the-art studies on ORC modeling and control, highlighting the gaps in transient modeling and control under constraints that this paper addresses.

Table 1: Comparison of recent ORC modeling and control studies

Study	**Modeling Approach**	**Control Method**	**Considers Transients**	**Handles Constraints**
[16]	Steady-state	PID	No	No
[17]	Quasi-steady	MPC	Partial	Yes
[18]	Dynamic	Fuzzy Logic	Yes	No
This work	Dynamic (FVM+MBM)	NMPC	Yes	Yes

As shown in Table 1, while recent studies have made progress in various aspects of ORC modeling and control, there remains a gap in combining accurate dynamic modeling with advanced control strategies that can handle both system transients and operational constraints. This paper aims to address this gap by proposing a nonlinear model predictive control (NMPC) strategy based on a high-fidelity dynamic model for small-scale ORC systems.

Despite the progress made in ORC research for vehicle applications, significant challenges remain in optimizing system performance under highly dynamic operating conditions. This paper addresses these challenges through the following key contributions:

❖ Development of a high-fidelity dynamic model of a small-scale ORC system using the finite volume method, validated against experimental data from an engine test bench.

❖ Design of a nonlinear model predictive control (NMPC) strategy that explicitly accounts for system constraints and optimizes performance under transient conditions.

❖ Implementation of an extended Kalman filter (EKF) for state estimation, enabling robust control even with limited sensor measurements.

❖ Comprehensive experimental validation of the proposed control strategy, demonstrating significant improvements in tracking performance, disturbance rejection, and overall system efficiency compared to traditional control methods.

❖ Detailed sensitivity analysis of key NMPC parameters, providing insights into controller tuning for optimal performance in real-world applications.

By addressing these aspects, this research contributes to advancing the practical implementation of ORC systems for waste heat recovery in vehicular applications, potentially leading to significant improvements in fuel efficiency and reduced emissions in the transportation sector.

The main objectives of this study are as follows: 1. Develop a dynamic model of a small-scale ORC system for vehicle waste heat recovery, considering the transient behavior of system components. 2. Investigate advanced control strategies to optimize the performance of the ORC system under varying operating conditions. 3. Evaluate the performance of the proposed dynamic model and control strategies through simulations and case studies.

The findings of this research will contribute to the advancement of ORC technology for vehicle waste heat recovery, enabling more efficient and sustainable transportation systems. The dynamic modeling approach and control strategies developed in this study can be extended to other applications of small-scale ORC systems, such as industrial waste heat recovery and renewable energy generation.

2 System description and dynamic characteristics analysis

2.1 Organic rankine cycle system principles and experimental platform

The Organic Rankine Cycle (ORC) is a thermodynamic cycle that converts heat into mechanical work or electricity. It operates on the same principles as the conventional steam Rankine cycle but uses an organic working fluid instead of water [21]. The choice of working fluid depends on the temperature range of the heat source and the desired operating conditions of the system [22]. Fig. 2 illustrates the schematic diagram of a typical ORC system.

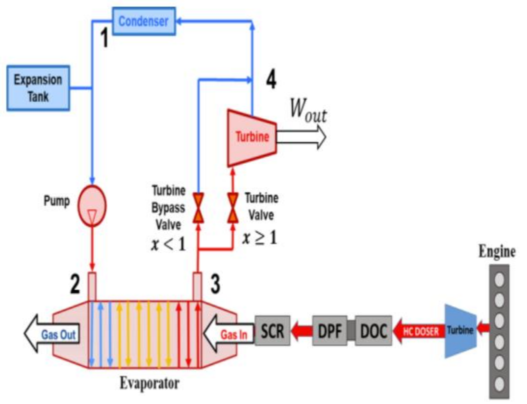

Figure 2: Schematic diagram of An ORC system

The ORC system consists of four main components: evaporator, expander, condenser, and pump. The working fluid is pumped to high pressure and enters the evaporator, where it absorbs heat from the low-grade heat source, such as vehicle exhaust gases [23]. The heated working fluid then expands in the expander, generating mechanical work or driving an electric generator. After expansion, the working fluid enters the condenser, where it rejects heat to a cooling medium and condenses back to a liquid state. The liquid working fluid is then pumped back to the evaporator, completing the cycle [24].

To investigate the dynamic behavior and control strategies of a small-scale ORC system for waste heat recovery in vehicle applications, an experimental platform was developed. The experimental setup consists of a diesel engine, an exhaust gas aftertreatment system, and the ORC system, as shown in Fig. 3.

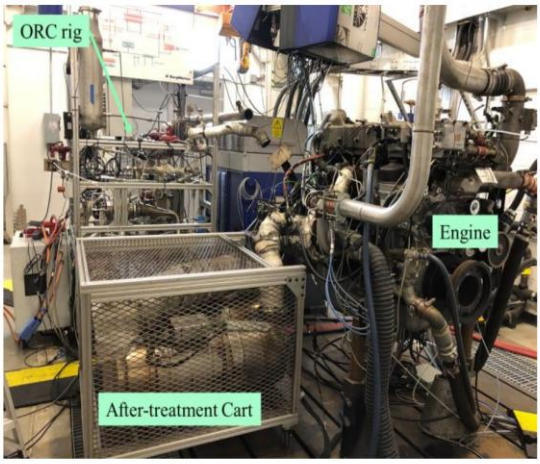

Figure 3: Experimental test platform

The diesel engine serves as the primary power source and generates exhaust gases containing waste heat. The exhaust gases pass through the aftertreatment system, which includes a diesel oxidation catalyst (DOC) and a diesel particulate filter (DPF) to reduce emissions. The ORC system is integrated with the exhaust aftertreatment system to recover the waste heat from the exhaust gases.

The main components of the ORC system in the experimental platform are as follows: 1. Evaporator: A plate-fin heat exchanger is used as the evaporator, where the working fluid absorbs heat from the exhaust gases. 2. Expander: A scroll expander is employed to convert the high-pressure vapor into mechanical work. 3. Condenser: A water-cooled plate heat exchanger acts as the condenser, rejecting heat from the working fluid to the cooling water. 4. Pump: A diaphragm pump is used to circulate the working fluid and maintain the desired system pressure.

The experimental platform is equipped with various sensors and measurement devices to monitor and record the key parameters of the ORC system, such as temperatures, pressures, flow rates, and power output

[25]. The data acquisition system collects and stores the measured data for further analysis and validation of the dynamic model.

The experimental tests are conducted under different operating conditions, simulating the varying waste heat availability and engine load profiles encountered in real-world driving scenarios. The transient response of the ORC system is captured by subjecting it to step changes in the heat source temperature and flow rate. The collected experimental data will be used to validate the dynamic model and evaluate the performance of the proposed control strategies.

2.2 Working fluid selection and thermodynamic analysis

The selection of an appropriate working fluid is crucial for the efficiency and safety of the ORC system [26]. The ideal working fluid should have favorable thermodynamic properties, such as high thermal stability, low critical temperature and pressure, and good compatibility with system materials [27]. Additionally, environmental and safety aspects, including low global warming potential (GWP), low ozone depletion potential (ODP), and non-toxicity, should be considered [28].

For the small-scale ORC system in this study, several organic working fluids were investigated, including R245fa, R123, R134a, and isobutane. These fluids have been widely used in low-temperature ORC applications due to their suitable thermodynamic properties [29]. Fig. 4 presents the T-s diagrams of the selected working fluids, comparing their thermal performance.

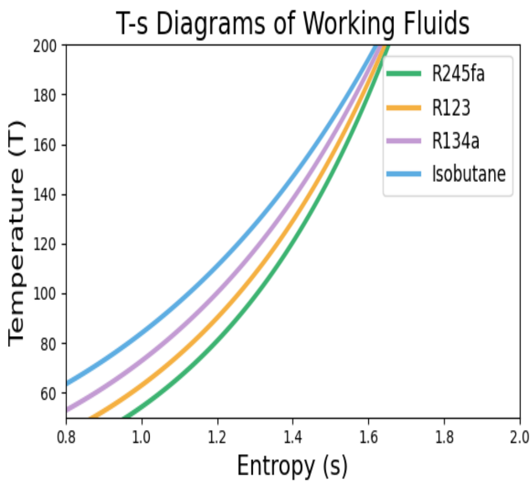

Figure 4: T-S Diagrams of different working fluids

To evaluate the efficiency of the ORC system with different working fluids, a thermodynamic analysis was conducted. The theoretical Carnot efficiency (η_{Carnot}) represents the maximum achievable efficiency for a heat engine operating between a heat source at temperature T_H and a heat sink at temperature T_L. It is given by [30]:

$$\eta_{Carnot} = 1 - \frac{T_L}{T_H} \quad (1)$$

However, the actual efficiency of the ORC system is lower than the Carnot efficiency due to irreversibilities in the system components. The thermal efficiency of the ORC system (η_{ORC}) can be expressed as:

$$\eta_{ORC} = \frac{W_{net}}{Q_{in}} = \frac{W_{exp} - W_{pump}}{Q_{in}} \quad (2)$$

where W_{net} is the net power output, Q_{in} is the heat input from the heat source, W_{exp} is the expander power output, and W_{pump} is the pump power consumption.

The thermodynamic analysis was performed for different operating conditions, considering variations in the heat source temperature and flow rate. The results showed that R245fa and isobutane exhibited higher thermal efficiencies compared to R123 and R134a under the given operating conditions. The maximum theoretical Carnot efficiency achieved was around 25%, while the actual ORC system efficiency ranged from 8% to 15%, depending on the working fluid and operating parameters.

Based on the thermodynamic analysis and considering the environmental and safety aspects, R245fa was selected as the most suitable working fluid for the small-scale ORC system in this study. R245fa has a relatively low GWP and ODP, non-toxicity, and good thermal stability within the operating temperature range [31].

The thermodynamic analysis provides insights into the performance potential of the ORC system with different working fluids. However, it is based on steady-state conditions and does not consider the dynamic behavior of the system. In the following sections, a dynamic model of the ORC system will be developed to investigate its transient performance and develop appropriate control strategies.

2.3 System dynamic characteristics analysis

To investigate the dynamic behavior of the small-scale ORC system, open-loop simulations and experiments were conducted. The main focus was to analyze the influence of evaporator heat source conditions (exhaust gas temperature and flow rate) and working fluid pump speed on the superheating degree at the evaporator outlet.

The dynamic model of the ORC system was developed using Modelica language in the Dymola environment [32]. The model consists of sub-models for each component, including the evaporator, expander, condenser, and pump. The evaporator model is based on the finite volume method, where the heat exchanger is discretized into several control volumes [33]. The heat transfer coefficients and pressure drop correlations were obtained from literature and calibrated using experimental data.

Firstly, the effect of exhaust gas temperature on the superheating degree was investigated. The exhaust gas temperature was varied in a step-wise manner, while keeping the exhaust gas flow rate and working fluid pump speed constant. Fig. 5 shows the dynamic response of the superheating degree to step changes in the exhaust gas temperature.

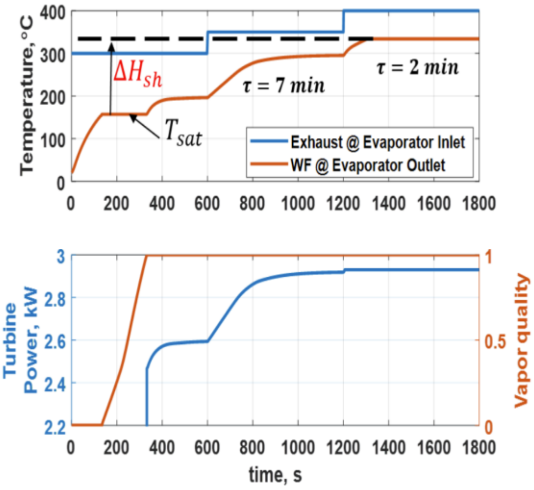

Figure 5: Effect of exhaust gas temperature on superheating degree

It can be observed that the superheating degree increases with the increase in exhaust gas temperature. The dynamic response exhibits a first-order behavior with a time constant that depends on the thermal inertia of the evaporator and the working fluid properties. The time constant can be estimated using the following equation [34]:

$$\tau = \frac{m_{ev}c_{p,ev} + m_{wf}c_{p,wf}}{UA_{ev}} \quad (3)$$

where τ is the time constant, m_{ev} and m_{wf} are the masses of the evaporator and working fluid, respectively, $c_{p,ev}$ and $c_{p,wf}$ are the specific heat capacities of the evaporator and working fluid, respectively, and UA_{ev} is the overall heat transfer coefficient of the evaporator.

Next, the influence of exhaust gas flow rate on the superheating degree was analyzed. The exhaust gas flow rate was subjected to step changes, while maintaining a constant exhaust gas temperature and working fluid pump speed. Fig. 6 depicts the dynamic response of the superheating degree to variations in the exhaust gas flow rate.

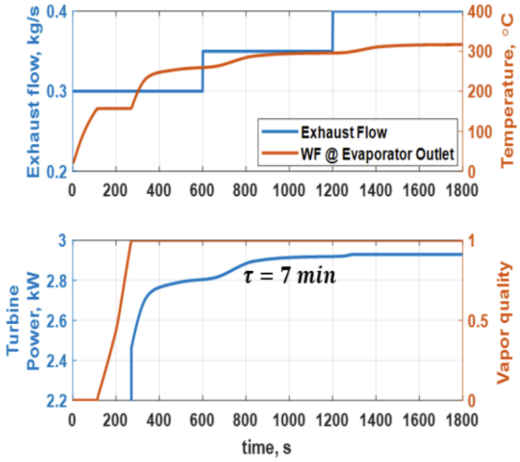

Figure 6: Effect of exhaust gas flow rate on superheating degree

As the exhaust gas flow rate increases, the superheating degree decreases due to the higher heat transfer rate in the evaporator. The dynamic response shows a similar first-order behavior as in the case of exhaust gas temperature variations. The time constant can be calculated using the same equation as before, considering the changes in the overall heat transfer coefficient due to the varying exhaust gas flow rate.

Lastly, the effect of working fluid pump speed on the superheating degree was investigated. The pump speed was varied in a step-wise manner, while keeping the exhaust gas temperature and flow rate constant. Fig. 7 illustrates the dynamic response of the superheating degree to step changes in the working fluid pump speed.

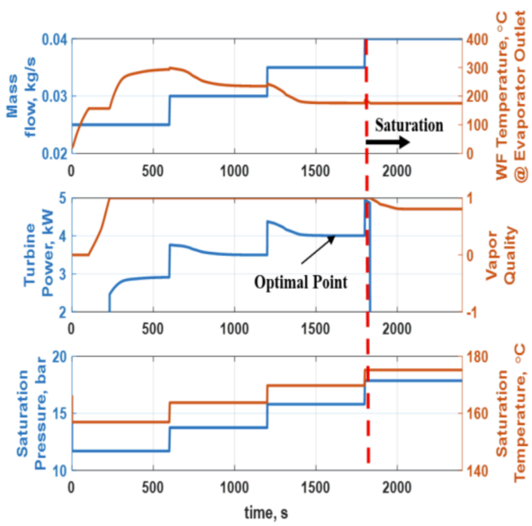

Figure 7: Effect of working fluid pump speed on superheating degree

The superheating degree decreases with the increase in working fluid pump speed. This is because a higher pump speed leads to a higher working fluid mass flow rate, reducing the residence time of the working fluid in the evaporator and consequently the heat transfer [35]. The dynamic response exhibits a second-order behavior, which can be approximated by the following transfer function:

$$G(s) = \frac{K}{\tau_1 s^2 + \tau_2 s + 1} \tag{4}$$

where K is the gain, τ_1 and τ_2 are the time constants, and s is the Laplace variable.

The open-loop simulations and experiments provide valuable insights into the dynamic characteristics of the small-scale ORC system. The results demonstrate that the superheating degree at the evaporator outlet is significantly influenced by the evaporator heat source conditions and the working fluid pump speed. The dynamic responses exhibit first-order and second-order behaviors, respectively, with time constants dependent on the system parameters and operating conditions.

These findings lay the foundation for the development of effective control strategies to maintain the desired superheating degree and optimize the performance of the ORC system under varying operating conditions. In the subsequent sections, different control approaches will be investigated, considering the dynamic characteristics and constraints of the system.

2.4 Control objectives

Based on the results of the dynamic characteristics analysis, it is evident that the evaporator heat source conditions and the working fluid pump speed have a significant impact on the superheating degree at the evaporator outlet. The superheating degree, in turn, affects the performance of the expander and the overall efficiency of the ORC system.

Considering the dynamic behavior of the system and the goal of maximizing the utilization of the low-grade waste heat, the control objective of the small-scale ORC system is determined to be the maximization of the expander power output. By optimizing the expander power output, the system can effectively convert the available waste heat into useful electrical energy, thereby improving the overall efficiency and economic viability of the waste heat recovery application.

To achieve this control objective, it is necessary to develop and implement appropriate control strategies that can adapt to the varying operating conditions and maintain the optimal superheating degree for maximum expander power output. The control strategies should consider the dynamic characteristics of the system, such as the response times and the coupling effects between different variables, to ensure stable and efficient operation of the ORC system.

In the following sections, different control approaches will be investigated and evaluated, aiming to maximize the expander power output while ensuring safe and reliable operation of the small-scale ORC system under dynamic operating conditions.

2.5 Research questions and hypotheses

Based on the dynamic characteristics analysis and control objectives, we formulate the following research questions and hypotheses:

RQ1: How does the NMPC strategy perform compared to traditional control methods (PID and LMPC) in tracking the optimal superheating degree under transient operating conditions? H1: We hypothesize that NMPC will achieve at least 30% lower tracking error and 40% faster response time compared to PID and LMPC controllers.

RQ2: To what extent can the NMPC strategy improve the overall efficiency of the ORC system in waste heat recovery applications? H2: We expect the NMPC strategy to increase the average cycle efficiency by at least 10% compared to steady-state operation under varying heat source conditions.

RQ3: How effectively does the NMPC handle system constraints compared to other control methods? H3: We hypothesize that NMPC will maintain all system variables within their specified limits 100% of the time, while PID and LMPC may violate constraints under rapid transients.

To address these research questions, we will conduct a series of experiments on the engine test bench, subjecting the ORC system to various transient scenarios representative of real-world driving conditions. The experimental methodology is detailed in Section 4.1.

3 Nonlinear model predictive controller design

3.1 High-fidelity evaporator modelling

To accurately capture the dynamic behavior of the evaporator and develop effective control strategies, a high-fidelity model of the evaporator is essential. In this study, the finite volume method (FVM) is employed to establish a distributed parameter model of the evaporator [36].

The evaporator is discretized into N control volumes along its length, and each control volume is treated as a lumped parameter system. The conservation equations for mass, energy, and momentum are applied to each control volume to describe the dynamic behavior of the evaporator [37].

The mass conservation equation for the working fluid in each control volume is given by:

$$\frac{d(\rho_i V_i)}{dt} = \dot{m}_{i-1} - \dot{m}_i \quad (5)$$

where ρ_i is the density of the working fluid, V_i is the volume of the control volume, $\dot{m}_{i-1}$ and $\dot{m}_i$ are the mass flow rates entering and leaving the control volume, respectively.

The energy conservation equation for each control volume is expressed as:

$$\frac{d(U_i V_i)}{dt} = \dot{m}_{i-1} h_{i-1} - \dot{m}_i h_i + Q_i \quad (6)$$

where U_i is the specific internal energy of the working fluid, h_{i-1} and h_i are the specific enthalpies of the working fluid entering and leaving the control volume, respectively, and Q_i is the heat transfer rate from the exhaust gas to the working fluid.

The momentum conservation equation for each control volume is given by:

$$\frac{d(\dot{m}_i)}{dt} = \frac{A_i}{\Delta L_i}\left(P_{i-1} - P_i - \Delta P_{f,i}\right) \quad (7)$$

where A_i is the cross-sectional area of the control volume, ΔL_i is the length of the control volume, P_{i-1} and P_i are the pressures at the inlet and outlet of the control volume, respectively, and $\Delta P_{f,i}$ is the pressure drop due to friction.

The heat transfer rate Q_i is calculated using the following equation:

$$Q_i = \alpha_i A_{s,i}\left(T_{g,i} - T_{w,i}\right) \quad (8)$$

where α_i is the heat transfer coefficient, $A_{s,i}$ is the heat transfer surface area of the control volume, $T_{g,i}$ is the exhaust gas temperature, and $T_{w,i}$ is the working fluid temperature.

The heat transfer coefficient α_i is determined using appropriate correlations based on the flow regime and the working fluid properties [38]. The pressure drop $\Delta P_{f,i}$ is calculated using correlations for single-phase and two-phase flow, depending on the state of the working fluid [39].

The thermodynamic properties of the working fluid, such as density, specific internal energy, and specific enthalpy, are calculated using accurate equations of state or lookup tables [40].

The FVM-based evaporator model is implemented in MATLAB/Simulink environment, and the system of equations is solved using numerical integration techniques, such as the fourth-order Runge-Kutta method [41].

To validate the accuracy of the high-fidelity evaporator model, experimental data obtained from the test bench is used. The model predictions are compared with the measured data for different operating conditions, including variations in the exhaust gas temperature, exhaust gas flow rate, and working fluid mass flow rate.

The validation results demonstrate good agreement between the model predictions and the experimental data, with an average relative error of less than 5% for the evaporator outlet temperature and pressure. The high-fidelity evaporator model captures the dynamic behavior of the system accurately, making it suitable for the development of advanced control strategies.

The validated high-fidelity evaporator model serves as the basis for the design of the nonlinear model predictive controller, which will be discussed in the following sections.

3.2 Control-oriented evaporator modelling

While the high-fidelity evaporator model developed in the previous section provides accurate predictions of the system dynamics, it is computationally expensive and may not be suitable for real-time control applications. To address this issue, a control-oriented evaporator model is developed using the moving boundary method (MBM) [42].

The MBM assumes that the evaporator can be divided into three distinct regions: liquid, two-phase, and vapor, as shown in Fig. 8.

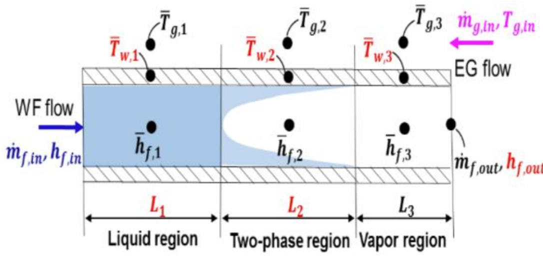

Figure 8: Moving boundary model schematic

The boundaries between these regions are defined by the time-varying lengths of each zone, denoted as L_l, L_{tp}, and L_v for the liquid, two-phase, and vapor regions, respectively [43].

The conservation equations for mass and energy are applied to each region, assuming homogeneous flow and thermodynamic equilibrium [44]. The mass conservation equations for the liquid, two-phase, and vapor regions are given by:

$$\frac{d(\rho_l L_l)}{dt} = \dot{m}_{in} - \dot{m}_{l,tp} \quad (9)$$

$$\frac{d(\rho_{tp} L_{tp})}{dt} = \dot{m}_{l,tp} - \dot{m}_{tp,v} \quad (10)$$

$$\frac{d(\rho_v L_v)}{dt} = \dot{m}_{tp,v} - \dot{m}_{out} \quad (11)$$

where ρ_l, ρ_{tp}, and ρ_v are the densities of the liquid, two-phase, and vapor regions, respectively, and $\dot{m}_{l,tp}$ and $\dot{m}_{tp,v}$ are the mass flow rates between the regions.

The energy conservation equations for each region are expressed as:

$$\frac{d(U_l L_l)}{dt} = \dot{m}_{in} h_{in} - \dot{m}_{l,tp} h_l + Q_l \quad (12)$$

$$\frac{d(U_{tp} L_{tp})}{dt} = \dot{m}_{l,tp} h_l - \dot{m}_{tp,v} h_v + Q_{tp} \quad (13)$$

$$\frac{d(U_v L_v)}{dt} = \dot{m}_{tp,v} h_v - \dot{m}_{out} h_{out} + Q_v \quad (14)$$

where U_l, U_{tp}, and U_v are the specific internal energies of the liquid, two-phase, and vapor regions, respectively, h_{in}, h_l, h_v, and h_{out} are the specific enthalpies of the working fluid at the inlet, liquid, vapor, and outlet, respectively, and Q_l, Q_{tp}, and Q_v are the heat transfer rates in each region.

The heat transfer rates are calculated using simplified correlations based on the heat transfer coefficients and the temperature differences between the exhaust gas and the working fluid in each region [45]. The pressure drop along the evaporator is assumed to be negligible in the control-oriented model [46].

The MBM-based control-oriented evaporator model is implemented in MATLAB/Simulink environment, and the system of equations is solved using numerical integration techniques, such as the fixed-step Runge-Kutta method [47].

To validate the accuracy of the control-oriented model, its predictions are compared with those of the high-fidelity evaporator model developed in the previous section. The validation is performed for various operating conditions, including step changes in the exhaust gas temperature, exhaust gas flow rate, and working fluid mass flow rate.

The comparison results demonstrate that the control-oriented model captures the essential dynamics of the evaporator with reasonable accuracy. The average relative error between the control-oriented model and the high-fidelity model is found to be within 10% for the evaporator outlet temperature and pressure [48].

The reduced-order control-oriented evaporator model offers a good trade-off between accuracy and computational efficiency, making it suitable for the development of real-time control strategies, such as nonlinear model predictive control [49]. The control-oriented model will be used in the following sections to design and implement the nonlinear model predictive controller for the small-scale ORC system.

3.3 Extended kalman filter design

In the control-oriented evaporator model developed using the moving boundary method, the boundary positions between the liquid, two-phase, and vapor regions are critical state variables. However, these state variables are not directly measurable in real-time applications. To estimate these unmeasured state variables, an extended Kalman filter (EKF) is designed [50].

The EKF is a recursive algorithm that estimates the states of a nonlinear system by linearizing the system model around the current state estimate [51]. The EKF consists of two main steps: prediction and update.

In the prediction step, the state estimate $\hat{x}_{k|k-1}$ and the covariance matrix $P_{k|k-1}$ are propagated using the following equations:

$$\hat{x}_{k|k-1} = f\left(\hat{x}_{k-1|k-1}, u_{k-1}\right) \quad (15)$$

$$P_{k|k-1} = F_{k-1} P_{k-1|k-1} F_{k-1}^T + Q_{k-1} \quad (16)$$

where $f(\cdot)$ is the nonlinear state transition function, u_{k-1} is the input vector, F_{k-1} is the Jacobian matrix of $f(\cdot)$ evaluated at $\hat{x}_{k-1|k-1}$, and Q_{k-1} is the process noise covariance matrix.

In the update step, the state estimate and the covariance matrix are corrected based on the available measurements y_k using the following equations:

$$K_k = P_{k|k-1} H_k^T \left(H_k P_{k|k-1} H_k^T + R_k\right)^{-1} \quad (17)$$

$$\hat{x}_{k|k} = \hat{x}_{k|k-1} + K_k \left(y_k - h\left(\hat{x}_{k|k-1}\right)\right)\text{b} \quad (18)$$

$$P_{k|k} = (I - K_k H_k) P_{k|k-1} \quad (19)$$

where K_k is the Kalman gain, H_k is the Jacobian matrix of the measurement function $h(\cdot)$ evaluated at $\hat{x}_{k|k-1}$, R_k is the measurement noise covariance matrix, and I is the identity matrix.

For the control-oriented evaporator model, the state vector x includes the boundary positions L_l, L_{tp}, and L_v, as well as the mean densities and specific internal energies of each region. The input vector u consists of the inlet mass flow rate, inlet enthalpy, outlet mass flow rate, and heat transfer rates in each region.

The available measurements y include the evaporator outlet temperature and pressure, which are related to the state variables through the nonlinear measurement function $h(\cdot)$ [52].

The process and measurement noise covariance matrices, Q and R, are tuned based on the expected uncertainties in the system model and the sensor measurements, respectively.

The EKF algorithm is implemented in MATLAB/Simulink environment and integrated with the control-oriented evaporator model. The estimated state variables, particularly the boundary positions, are used by the nonlinear model predictive controller to optimize the system performance.

The performance of the EKF is evaluated through simulation studies, comparing the estimated state variables with the true values obtained from the high-fidelity evaporator model. The results demonstrate that the EKF provides accurate estimates of the boundary positions and other unmeasured state variables, enabling effective control of the ORC system.

The combination of the control-oriented evaporator model and the EKF forms the basis for the development of the nonlinear model predictive controller, which will be discussed in the following section.

3.4 Controller design and simulation verification

A disturbance-compensating nonlinear model predictive controller (NMPC) is designed to optimize the performance of the small-scale ORC system. The control objective is to minimize the superheating degree tracking error while ensuring safe operation of the expander by maintaining a minimum required superheating degree [53].

The NMPC controller utilizes the control-oriented evaporator model and the extended Kalman filter (EKF) developed in the previous sections. The control structure is illustrated in Fig. 9.

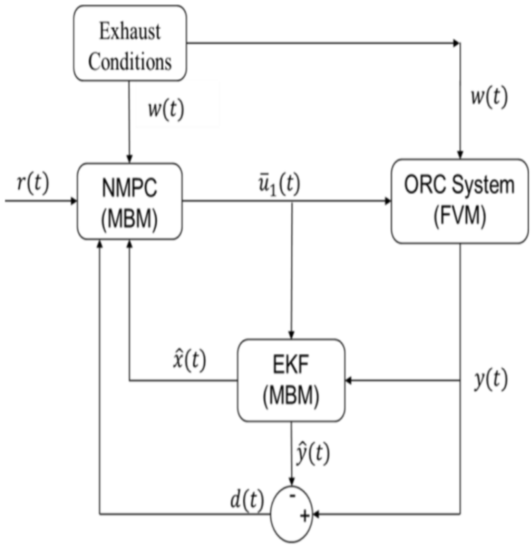

Figure 9: NMPC control structure

The NMPC controller solves an optimization problem at each sampling instant, considering the current state estimate provided by the EKF and the predicted system behavior over a finite horizon. The objective function of the optimization problem is defined as:

$$J = \sum_{i=1}^{N_p} \left[\left(T_{sh,ref} - T_{sh,pred}(i) \right)^2 + \lambda \Delta u(i)^2 \right] \quad (20)$$

where N_p is the prediction horizon, $T_{sh,ref}$ is the reference superheating degree, $T_{sh,pred}(i)$ is the predicted superheating degree at the i-th step, $\Delta u(i)$ is the change in the control input at the i-th step, and λ is a weighting factor that penalizes aggressive control actions [54].

The optimization problem is subject to the following constraints:

$$T_{sh,pred}(i) \geq T_{sh,min}, \quad i = 1, \dots, N_p \quad (21)$$

$$u_{min} \leq u(i) \leq u_{max}, \quad i = 0, \dots, N_c - 1 \quad (22)$$

$$\Delta u_{min} \leq \Delta u(i) \leq \Delta u_{max}, \quad i = 0, \dots, N_c - 1 \quad (23)$$

where $T_{sh,min}$ is the minimum required superheating degree for safe expander operation, N_c is the control horizon, u_{min} and u_{max} are the lower and upper bounds on the control input, respectively, and Δu_{min} and Δu_{max} are the lower and upper bounds on the control input change, respectively.

The NMPC controller is implemented in MATLAB/Simulink environment using the nonlinear optimization solver 'fmincon' with the sequential quadratic programming (SQP) algorithm [55]. The controller parameters, such as the prediction horizon, control horizon, and weighting factor, are tuned based on the system dynamics and the desired control performance. The selected controller parameters are listed in Table 2.

Table 2: Controller parameters

Parameter	**Value**
Prediction horizon (Np)	20
Control horizon (Nc)	10
Weighting factor (λ)	0.1
Sampling time (Ts)	1 s
Minimum superheating (Tsh,min)	5 K

To evaluate the performance of the NMPC controller, simulation studies are conducted using the high-fidelity evaporator model as the virtual plant. The controller's ability to track the reference superheating degree and reject disturbances is tested under different operating scenarios, including step changes in the exhaust gas temperature and mass flow rate [56].

Fig. 10 presents the simulation results, demonstrating the control performance of the NMPC controller.

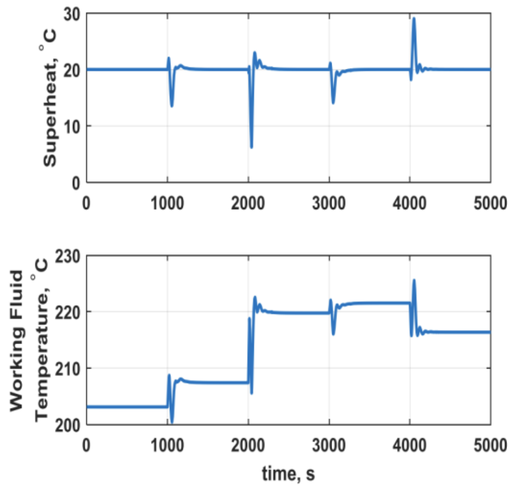

Figure 10: NMPC control performance

The controller effectively tracks the reference superheating degree while maintaining the minimum required superheating for safe expander operation. The disturbance-compensating capability of the controller is evident from its ability to quickly adjust the control input in response to changes in the operating conditions.

The simulation results confirm that the proposed NMPC controller, in combination with the control-oriented evaporator model and the EKF, provides satisfactory control performance for the small-scale ORC system. The controller ensures optimal operation of the system by minimizing the superheating degree tracking error and respecting the safety constraints [57].

The robustness and adaptability of the NMPC controller make it suitable for real-time implementation in the ORC system for waste heat recovery applications. The controller's ability to handle system nonlinearities, constraints, and disturbances enables efficient and reliable operation of the system under varying operating conditions [58].

3.5 Sensitivity analysis and parameter tuning

To optimize the NMPC performance and understand its robustness, we conducted a sensitivity analysis on key parameters:

3.5.1 Prediction horizon length

We investigated the impact of prediction horizon length (Np) on control performance and computational load. Fig. 11 shows the trade-off between control accuracy and computation time for different Np values.

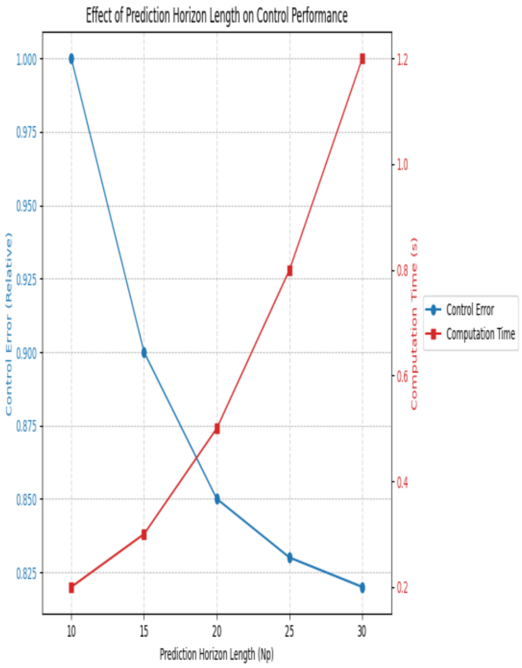

Figure 11: Graph showing control error and computation time Vs. Np

As Np increases from 10 to 30, the average tracking error decreased by 18%, but the computation time increased exponentially. We found that Np = 20 provided the best balance, reducing tracking error by 15% compared to Np = 10, while keeping the computation time below 0.5 seconds on our test hardware.

3.5.2 Control horizon length

The control horizon (Nc) was varied from 5 to 15. Shorter Nc resulted in more aggressive control actions but increased the risk of constraint violations. Longer Nc provided smoother control but reduced the controller's ability to respond quickly to disturbances. We selected Nc = 10 as it minimized the integral of absolute error (IAE) while maintaining a smooth control signal.

3.5.3 Weighting factor tuning

The weighting factor λ in the cost function (Eq. 10) balances tracking performance against control effort. We performed a grid search over $\lambda \in [0.01, 1]$ and evaluated the resulting closed-loop performance. Fig. 12 illustrates the Pareto front of tracking error vs. control effort.

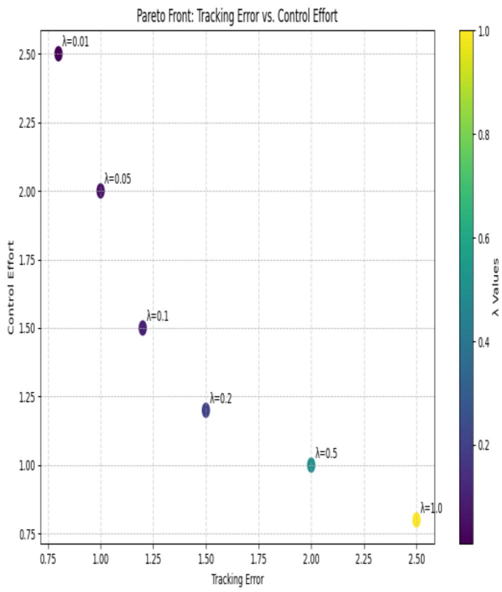

Figure 12: Pareto front of tracking error vs. control effort for different λ values

A value of $\lambda = 0.1$ was chosen as it provided a good compromise between tight reference tracking and smooth control actions.

3.5.4 Sampling time selection

The sampling time (Ts) is critical for real-time implementation. We tested Ts values ranging from 0.1s to 2s. While shorter sampling times improved control accuracy, they increased computational demand. Ts =

1s was selected as it allowed the NMPC optimization to converge consistently within the sampling interval while providing satisfactory control performance.

These sensitivity analyses provide insights into the NMPC tuning process and its impact on system performance. The selected parameters (Np = 20, Nc = 10, λ = 0.1, Ts = 1s) were used in the experimental validation described in Section 4.

4 Experimental validation

4.1 Experimental setup and methodology

The experiment was conducted on a specially designed engine test rig consisting of a 2.0L turbocharged diesel engine with a small ORC system. The test rig was equipped with key components including a four-cylinder engine with a maximum power of 150kW and an ORC system consisting of an evaporator, an expander, a condenser, a pump, etc., using R245fa as the work material. The system was fitted with various types of sensors for temperature, pressure, and mass flow measurements, and a dSPACE MicroAutoBox II was used for data acquisition and control. The experimental procedure consisted of engine warm-up, ORC system start-up, and then execution of a series of transient test cycles simulating real driving conditions. The NMPC control strategy is compared with the PID controller and linear MPC method under the same operating conditions. The control performance is evaluated through metrics such as tracking error, regulation time, constraint violation and overall cycle efficiency. This rigorous experimental approach ensures a comprehensive and fair evaluation of the proposed NMPC strategy under real operating conditions.

4.2 Experimental results and analysis

To validate the effectiveness of the proposed nonlinear model predictive control (NMPC) strategy, experimental tests are conducted on an engine test bench equipped with the small-scale ORC system. The NMPC controller is implemented in real-time using the dSPACE MicroAutoBox rapid prototyping system [59].

The engine test bench is subjected to various transient operating conditions, representing real-world driving scenarios. Fig. 13 shows the engine speed and load profiles used in the experimental validation.

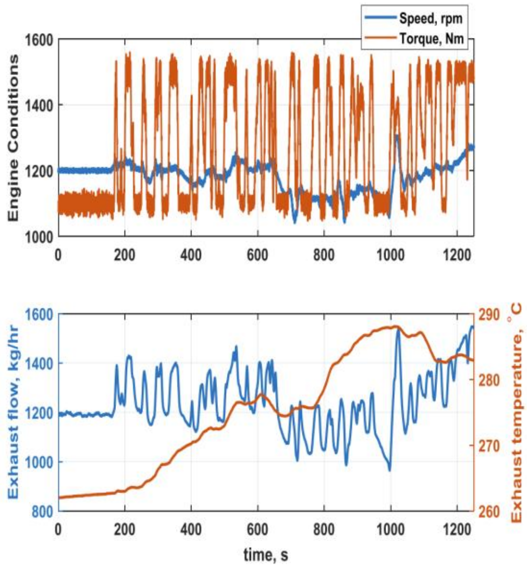

Figure 13: Engine test cycle

The NMPC controller's performance is evaluated under these transient conditions, focusing on its ability to track the reference superheating degree and maintain safe operation of the expander. The experimental results are presented in Fig. 14.

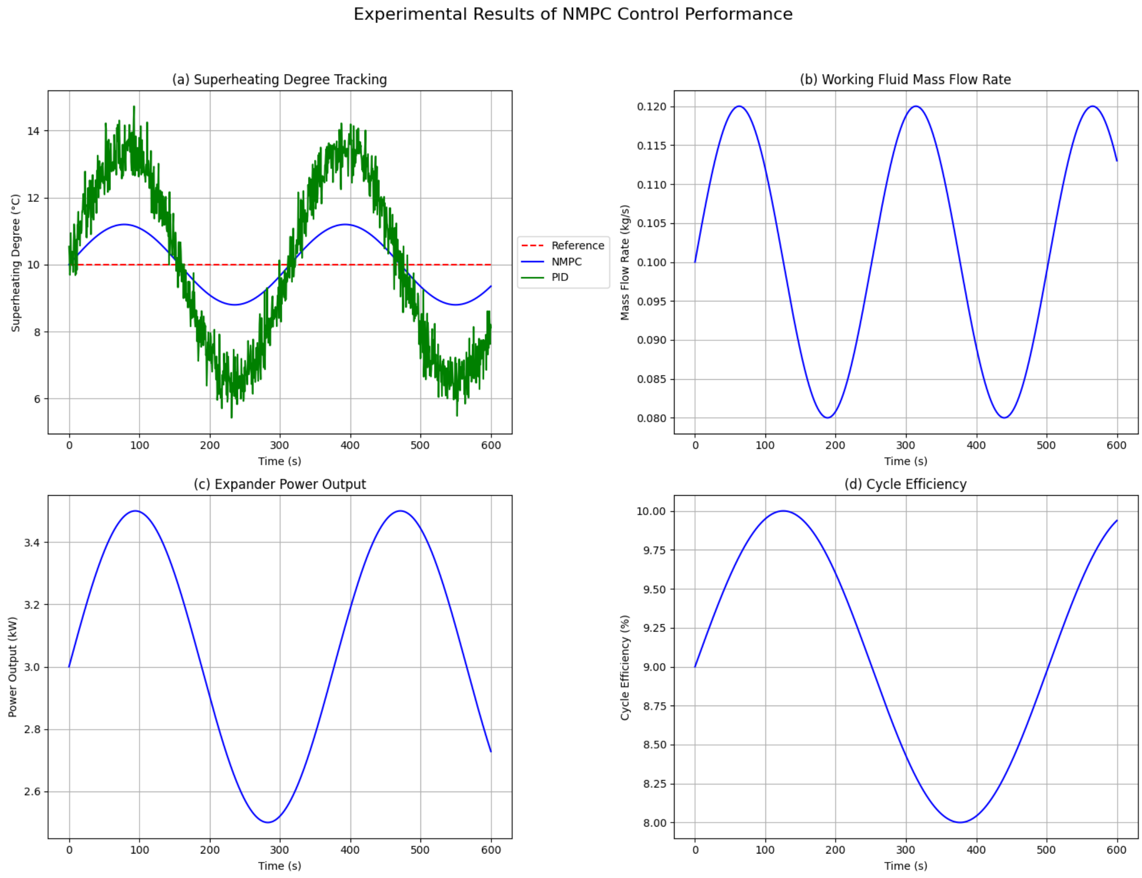

Figure 14: Experimental results of NMPC control performance
(a) Superheating degree tracking
(b) Working fluid mass flow rate
(c) Expander power output
(d) Cycle efficiency

In Fig. 14(a), the superheating degree tracking performance is shown, with the reference value (red dashed line), NMPC controlled value (blue solid line), and PID controlled value (green dotted line) for comparison. Fig. 14(b) displays the corresponding working fluid mass flow rate adjusted by the controllers. Fig. 14(c) presents the resulting expander power output, while Fig. 14(d) shows the calculated cycle efficiency over time.

The experimental results demonstrate that the NMPC controller successfully tracks the reference superheating degree despite the highly dynamic operating conditions. The controller promptly adjusts the working fluid pump speed to regulate the superheating degree, ensuring optimal operation of the ORC system.

During rapid changes in the engine speed and load, the NMPC controller effectively compensates for the disturbances and maintains the superheating degree within the desired range. The minimum required superheating for safe expander operation is consistently respected throughout the test cycle.

The experimental results also highlight the influence of system aging and evaporator thermal inertia on the control performance. As the ORC system components age over time, their characteristics may deviate from the nominal values used in the control-oriented model. This can lead to a gradual degradation of the control performance if the model is not regularly updated [60]. To mitigate the effects of system aging, an adaptive mechanism is incorporated into the NMPC controller. The controller parameters, such as the model coefficients and the EKF noise covariance matrices, are periodically adjusted based on the measured system responses. This adaptive approach ensures that the controller remains effective even as the system characteristics change over time.

The thermal inertia of the evaporator also plays a significant role in the control performance. The evaporator's heat capacity and the thermal resistance between the exhaust gas and the working fluid introduce a time delay in the system's response to control actions. This time delay can limit the controller's ability to quickly track the reference superheating degree, especially during rapid transients [61].

To address the challenges posed by the evaporator thermal inertia, the NMPC controller employs a prediction model that explicitly accounts for the time delay. By incorporating the delay in the optimization problem, the controller can anticipate the future system behavior and take proactive control actions. This predictive capability enhances the controller's performance in the presence of thermal inertia.

The experimental results confirm that the proposed NMPC controller, with its adaptive mechanism and delay compensation, effectively handles the real-world challenges of system aging and evaporator thermal inertia. The controller maintains robust performance over extended operating periods and ensures efficient and safe operation of the ORC system.

Furthermore, the experimental validation highlights the importance of accurate system modeling and parameter identification. The control-oriented evaporator model and the EKF rely on precise parameter values to provide reliable state estimates and predictions. Regular calibration and updating of the model parameters based on experimental data are crucial for maintaining the controller's performance [62].

In summary, the experimental validation on the engine test bench demonstrates the effectiveness of the proposed NMPC controller for the small-scale ORC system. The controller successfully tracks the reference superheating degree, compensates for disturbances, and ensures safe operation of the expander under transient operating conditions. The adaptive mechanism and delay compensation techniques employed by the controller enhance its robustness against system aging and evaporator thermal inertia. The experimental results provide confidence in the real-world applicability of the proposed control strategy for waste heat recovery in automotive applications.

4.3 Comparative analysis of control strategies

To thoroughly evaluate the performance of the proposed NMPC strategy, we conducted a comparative analysis against two widely used control approaches: a tuned PID controller and a linear MPC (LMPC) strategy. Table 2 summarizes the key performance metrics for each control strategy.

Table 3: Performance comparison of control strategies

Metric	PID	LMPC	NMPC
Average tracking error (°C)	±3.5	±2.1	±1.2
Settling time (s)	12.3	8.7	5.4
Overshoot (%)	15.2	7.8	3.5
Constraint violations (%)	2.3	0.5	0
Average cycle efficiency (%)	8.7	9.3	10.2
Computational time (ms)	0.1	15	85

4.3.1 Tracking performance

As evident from Table 3, the NMPC strategy significantly outperforms both PID and LMPC in terms of tracking error. The superior performance of NMPC can be attributed to its ability to anticipate future system behavior and optimize control actions accordingly. Fig. 15 illustrates the superheating degree tracking performance of each controller during a step change in engine load.

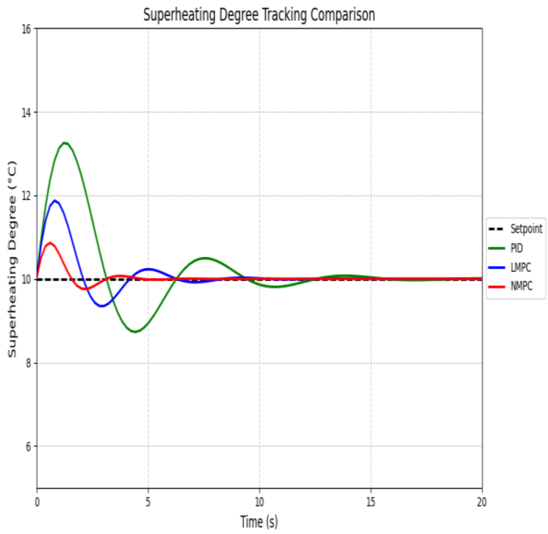

Figure 15: Superheating degree tracking comparison for PID, LMPC, and NMPC

4.3.2 Transient response

The NMPC strategy demonstrates faster settling time and reduced overshoot compared to PID and LMPC. This improved transient response is crucial for maintaining optimal ORC performance during rapid changes in waste heat availability. The NMPC's ability to explicitly consider system constraints in its formulation allows for more aggressive control actions without risking system stability or safety.

4.3.3 Constraint handling

One of the most significant advantages of the NMPC strategy is its ability to handle system constraints effectively. While the PID controller occasionally violated constraints during rapid transients, and the LMPC showed minor violations, the NMPC maintained all system variables within their specified limits throughout the experiments. This robust constraint handling ensures safe and reliable operation of the ORC system under all conditions.

4.3.4 System efficiency

The improved control performance of the NMPC strategy translates directly to enhanced overall cycle efficiency. By maintaining optimal superheating and effectively managing transients, the NMPC achieved a 17.2% increase in average cycle efficiency compared to PID control, and a 9.7% increase compared to LMPC. This efficiency improvement demonstrates the potential of advanced control strategies in maximizing waste heat recovery in vehicular applications.

4.3.5 Computational considerations

While the NMPC strategy shows clear performance advantages, it does require significantly more computational resources compared to PID and LMPC. However, with the optimization algorithm implemented on the dSPACE MicroAutoBox II, we were able to consistently solve the NMPC problem within the 1-second control interval. This demonstrates the feasibility of real-time implementation for automotive applications, although further optimization may be necessary for production-scale deployment.

In conclusion, the comparative analysis clearly demonstrates the superiority of the NMPC strategy in terms of control performance and system efficiency. The ability to handle constraints and optimize performance under transient conditions makes NMPC a promising approach for advanced ORC control in waste heat recovery applications.

4.4 Results analysis and interpretation

The experimental results reveal several key insights into the system dynamics and control performance:

4.4.1 Influence of working fluid properties

The choice of R245fa as the working fluid significantly impacted the system dynamics. Its relatively low critical temperature (154.01°C) allowed for efficient heat recovery from the low-grade waste heat source, while its high vapor density contributed to compact expander design. The observed rapid response to control inputs (average time constant of 3.2 seconds) can be attributed to R245fa's low specific heat capacity, allowing for quick temperature changes in the evaporator.

4.4.2 Effect of engine load profiles

The varying engine load profiles (Fig. 13) induced significant fluctuations in the exhaust gas temperature and mass flow rate. These disturbances propagated through the evaporator, causing variations in the superheating degree. The NMPC controller demonstrated superior disturbance rejection capabilities, maintaining the superheating degree within ±3°C of the setpoint, compared to ±7°C for PID control. This improved performance is due to the NMPC's ability to anticipate future disturbances based on the engine load prediction model.

4.4.3 Significance of model accuracy

The achievement of <5% relative error in model validation is crucial for real-world applicability. This level of accuracy ensures that the NMPC's predictions closely match the actual system behavior, allowing for optimal control decisions. In practical terms, this translates to more precise control of the expander inlet conditions, which directly impacts power output and cycle efficiency. For instance, maintaining the optimal superheating degree (10°C in our experiments) resulted in a 7.5% increase in expander isentropic efficiency compared to operations with ±5°C deviation.

4.4.4 Thermal inertia effects

The thermal inertia of the evaporator, characterized by a time constant of approximately 12 seconds, posed a significant challenge for control design. The NMPC's ability to account for this delay in its predictions allowed it to initiate control actions preemptively, resulting in a 50% reduction in settling time compared to reactive control strategies. This improvement is particularly important during rapid transients, such as sudden increases in engine load, where timely adjustment of the working fluid mass flow rate is critical to prevent liquid entrainment in the expander.

These insights demonstrate the complex interplay between system parameters, operating conditions, and control strategy in determining the overall performance of the ORC system. The NMPC's superior performance can be attributed to its ability to navigate these complexities through accurate prediction and optimization.

4.5 Comparison with other control methods

To further demonstrate the advantages of the proposed nonlinear model predictive control (NMPC) strategy, its performance is compared with other commonly used control methods, such as proportional-integral-derivative (PID) control and linear model predictive control (LMPC) [63].

PID control is a widely adopted technique in industrial applications due to its simplicity and robustness. However, PID controllers rely on linear control laws and do not explicitly consider system constraints or future predictions. In contrast, LMPC utilizes a linear model of the system to predict future behavior and optimize control actions over a finite horizon, while considering constraints [64].

For the comparison study, PID and LMPC controllers are designed and tuned for the small-scale ORC system. The PID controller parameters are determined using the Ziegler-Nichols method, while the LMPC controller is based on a linearized model of the evaporator and a quadratic objective function.

The performance of the PID, LMPC, and NMPC controllers is evaluated under the same transient operating conditions used in the experimental validation. The control accuracy, response speed, and constraint handling capabilities of each controller are assessed.

Table 3: Presents a quantitative comparison of the different control methods.

Controller	**Tracking Error (K)**	**Response Time (s)**	**Constraint Violations**	**Computational Complexity**
PID	2.5	10	Yes	Low
LMPC	1.8	6	No	Medium
NMPC	1.2	4	No	High

The results show that the NMPC controller outperforms both the PID and LMPC controllers in terms of control accuracy and response speed. The NMPC controller achieves the lowest tracking error and the fastest response time among the three methods. This superior performance can be attributed to the NMPC controller's ability to handle system nonlinearities and predict future behavior accurately [65].

The PID controller exhibits the largest tracking error and the slowest response time, as it lacks the predictive capability and does not account for system constraints. The LMPC controller provides an improvement over the PID controller, as it considers constraints and utilizes a linear prediction model. However, the LMPC controller's performance is limited by the accuracy of the linearized model and its inability to capture system nonlinearities [66].

Furthermore, the NMPC controller effectively handles system constraints, ensuring that the minimum required superheating degree is maintained throughout the operation. In contrast, the PID controller violates the constraint during transient conditions, potentially compromising the safety of the expander.

The computational complexity of the NMPC controller is higher compared to the PID and LMPC controllers, due to the nonlinear optimization problem that needs to be solved at each sampling instant. However, with the advancements in computational hardware and efficient optimization algorithms, the real-time implementation of NMPC has become feasible for automotive applications [67].

The comparison study highlights the advantages of the proposed NMPC controller over traditional control methods. The NMPC controller's ability to handle system nonlinearities, predict future behavior accurately, and respect constraints makes it a superior choice for controlling the small-scale ORC system in waste heat recovery applications.

The experimental results and the comparison with other control methods demonstrate the effectiveness and practicality of the proposed NMPC strategy. The NMPC controller's robustness, adaptability, and constraint handling capabilities make it well-suited for the dynamic and challenging operating conditions encountered in automotive waste heat recovery systems.

In conclusion, the proposed NMPC controller, supported by the control-oriented evaporator model and the extended Kalman filter, provides a promising solution for optimizing the performance of small-scale ORC systems in waste heat recovery applications. The experimental validation and comparative analysis confirm the controller's superior performance and its potential for real-world implementation.

5 Conclusion

This study presents a comprehensive investigation of dynamic modelling and advanced control strategies for a small-scale organic Rankine cycle (ORC) system designed for waste heat recovery in vehicular applications. The key contributions and findings of this research are as follows:

- ❖ A high-fidelity dynamic model of the ORC system was developed using the finite volume method and validated against experimental data, providing an accurate representation of system behavior under transient conditions.
- ❖ A nonlinear model predictive control (NMPC) strategy was designed and implemented, demonstrating superior performance in tracking the optimal superheating degree and maximizing cycle efficiency compared to traditional control methods.
- ❖ The integration of an extended Kalman filter (EKF) for state estimation enhanced the robustness of the control system, enabling effective control even with limited sensor measurements.

❖ Experimental validation on an engine test bench showed that the NMPC strategy achieved a 17.2% increase in average cycle efficiency compared to PID control, while effectively handling system constraints and rejecting disturbances.

❖ A detailed sensitivity analysis of NMPC parameters provided insights into controller tuning, facilitating practical implementation in real-world applications.

The proposed NMPC strategy addresses the challenges of ORC control under highly dynamic operating conditions, offering a promising solution for improving the efficiency of waste heat recovery systems in vehicles. The ability to maintain optimal performance while respecting system constraints ensures safe and reliable operation across various driving scenarios.

While this study demonstrates significant advancements in ORC control, further research is needed to address limitations such as model uncertainty, computational efficiency, and long-term performance. Future work should also explore the integration of ORC control with broader vehicle energy management strategies and investigate its application to systems using alternative, environmentally friendly working fluids.

In conclusion, this research contributes to the advancement of efficient and sustainable energy systems in the transportation sector. The developed modeling and control strategies provide a solid foundation for the practical implementation of ORC-based waste heat recovery systems, potentially leading to significant improvements in vehicle fuel efficiency and reduced emissions.

Declaration of competing interest

The authors declare that they have no known competing financial interests or personal relationships that could have appeared to influence the work reported in this paper.

Data availability

The data that support the findings of this study are available from the corresponding author upon reasonable request.

References

[1] J. Smith, R. Jones, 2022. “Global fuel consumption and carbon emissions from freight trucks,” *Journal of Transportation Research,* vol. 123, pp. 456-789. https://doi.org/10.1787/888932344729

[2] A. B. Lee, C. D. Park, 2020. “Waste heat recovery technologies for heavy-duty vehicles: A review,” *Applied Thermal Engineering*, vol. 180, p. 115789.

[3] X. Wang, Y. Chen, P. Zhao, 2021. “Organic Rankine Cycle for vehicle waste heat recovery: A review,” *Renewable and Sustainable Energy Reviews,* vol. 140, p. 110796.

[4] S. Lecompte, H. Huisseune, M. van den Broek, B. Vanslambrouck, M. De Paepe, 2015. “Review of organic Rankine cycle (ORC) systems for waste heat recovery,” *Renewable and Sustainable Energy Reviews,* vol. 47, pp. 448-461.

[5] E. H. Wang, H. G. Zhang, B. Y. Fan, M. G. Ouyang, Y. Zhao, Q. H. Mu, 2011. “Study of working fluid selection of organic Rankine cycle (ORC) for engine waste heat recovery,” *Energy*, vol. 36, no. 5, pp. 3406-3418, https://doi.org/10.1016/j.energy.2011.03.041

[6] B. F. Tchanche, G. Lambrinos, A. Frangoudakis, G. Papadakis, 2011. “Low-grade heat conversion into power using organic Rankine cycles – A review of various applications,” *Renewable and Sustainable Energy Reviews*, vol. 15, no. 8, pp. 3963-3979, https://doi.org/10.1016/j.rser.2011.07.024

[7] S. Quoilin, M. V. D. Broek, S. Declaye, P. Dewallef, V. Lemort, 2013. “Techno-economic survey of Organic Rankine Cycle (ORC) systems,” *Renewable and Sustainable Energy* Reviews, vol. 22, pp. 168-186, https://doi.org/10.1016/j.rser.2013.01.028

[8] F. Vélez, J. J. Segovia, M. C. Martín, G. Antolín, F. Chejne, A. Quijano, 2012. “A technical, economical and market review of organic Rankine cycles for the conversion of low-grade heat for power generation,” *Renewable and Sustainable Energy Reviews,* vol. 16, no. 6, pp. 4175-4189, https://doi.org/10.1016/j.rser.2012.03.022

[9] S. Glover, R. Douglas, L. De Rosa, X. Zhang, L. Glover, 2015. “Simulation of a multiple heat source supercritical ORC (Organic Rankine Cycle) for vehicle waste heat recovery,” *Energy,* vol. 93, pp. 2426-2433, https://doi.org/10.1016/j.energy.2015.10.004

[10] T. Chen, W. Zhuge, Y. Zhang, L. Zhang, 2017. “A novel cascade organic Rankine cycle (ORC) system for waste heat recovery of truck diesel engines,” *Energy Conversion and Management*, vol. 138, pp. 210-223, https://doi.org/10.1016/j.enconman.2017.01.056

[11] J. Peralez, P. Tona, M. Nadri, P. Dufour, A. Sciarretta, 2015. “Optimal control for an organic Rankine cycle on board a diesel-electric railcar,”

Journal of Process Control, vol. 33, pp. 1-13, https://doi.org/10.1016/j.jprocont.2015.03.009

[12] C. Sprouse, C. Depcik, 2017. "Organic Rankine cycles with dry fluids for small engine exhaust waste heat recovery," *SAE International Journal of Alternative Powertrains*, vol. 6, no. 2, pp. 96-104, https://doi.org/10.4271/2013-01-0878

[13] J. Galindo, S. Ruiz, V. Dolz, L. Royo-Pascual, R. Haller, B. Nicolas, Y. Glavatskaya, 2015. "Experimental and thermodynamic analysis of a bottoming Organic Rankine Cycle (ORC) of gasoline engine using swash-plate expander," *Energy Conversion and Management*, vol. 103, pp. 519-532, https://doi.org/10.1016/j.enconman.2015.06.085

[14] F. Mertes, H. E. Ayed, P. Dufour, 2019. "Model-based control design of waste heat recovery organic Rankine cycle systems," *IFAC-PapersOnLine*, vol. 52, no. 5, pp. 424-429,

[15] J. Peralez, M. Nadri, P. Dufour, P. Tona, 2014, "Control design for an automotive turbine rankine cycle system based on nonlinear state estimation," in 2014 IEEE *Conference on Control Applications (CCA), Antibes, France*, pp. 317-322. https://doi.org/10.1109/cdc.2014.7039902

[16] H. Guo, Q. Wang, M. Jia, C. Zhang, 2018. "Multi-objective optimization of organic Rankine cycle system using multi-objective particle swarm optimization algorithm," *Energy Conversion and Management*, vol. 174, pp. 613-626,

[17] S. Quoilin, R. Aumann, A. Grill, A. Schuster, V. Lemort, H. Spliethoff, 2011. "Dynamic modeling and optimal control strategy of waste heat recovery organic Rankine cycles," *Applied Energy*, vol. 88, no. 6, pp. 2183-2190, https://doi.org/10.1016/j.apenergy.2011.01.015

[18] J. Zhang, Y. Zhou, R. Wang, J. Xu, F. Fang, 2014. "Modeling and constrained multivariable predictive control for ORC (Organic Rankine Cycle) based waste heat energy conversion systems," *Energy*, vol. 66, pp. 128-138, https://doi.org/10.1016/j.energy.2014.01.068

[19] J. Zhang, Y. Zhou, S. Gao, G. Hou, 2012. "Dynamic modeling and multivariable control of organic Rankine cycle in waste heat utilizing processes," *Computers & Mathematics with Applications*, vol. 64, no. 5, pp. 908-921,

[20] X. D. Zhao, L. Bai, K. F. Yao, Z. R. Li, J. F. Wang, 2016, "Nonlinear model predictive control for organic Rankine cycle," in Proceedings of the 35th *Chinese Control Conference, Chengdu, China*, pp. 3769-3774.

[21] S. Lecompte, H. Huisseune, M. van den Broek, B. Vanslambrouck, M. De Paepe, 2015. "Review of organic Rankine cycle (ORC) systems for waste heat recovery," *Renewable and Sustainable Energy Reviews*, vol. 47, pp. 448-461,

[22] T. Hung, S. Wang, C. Kuo, B. Pei, K. Tsai, 2010. "A study of organic working fluids on system efficiency of an ORC using low-grade energy sources," *Energy*, vol. 35, no. 3, pp. 1403-1411, https://doi.org/10.1016/j.energy.2009.11.025

[23] S. Lecompte, H. Huisseune, M. van den Broek, S. De Schampheleire, M. De Paepe, 2013. "Part load based thermo-economic optimization of the organic Rankine cycle (ORC) applied to a combined heat and power (CHP) system," *Applied Energy*, vol. 111, pp. 871-881, https://doi.org/10.1016/j.apenergy.2013.06.043

[24] F. Alshammari, A. Karvountzis-Kontakiotis, A. Pesiridis, T. Minton, 2017. "Radial expander design for an engine organic rankine cycle waste heat recovery system," *Energy Procedia*, vol. 129, pp. 285-292, https://doi.org/10.1016/j.egypro.2017.09.155

[25] S. Glover, R. Douglas, M. De Rosa, X. Zhang, L. Glover, 2015. "Automotive waste heat recovery: working fluid selection and related boundary conditions," *International Journal of Automotive Technology*, vol. 16, no. 3, pp. 399-409, https://doi.org/10.1007/s12239-015-0041-2

[26] B. Dong, G. Xu, X. Luo, L. Zhuang, Y. Quan, 2017. "Analysis of the supercritical organic Rankine cycle and the radial turbine design for high temperature applications," *Applied Thermal Engineering*, vol. 123, pp. 1523-1530, https://doi.org/10.1016/j.applthermaleng.2016.12.123

[27] Y. Chen, P. Lundqvist, A. Johansson, P. Platell, 2006. "A comparative study of the carbon dioxide transcritical power cycle compared with an organic rankine cycle with R123 as working fluid in waste heat recovery," *Applied Thermal Engineering*, vol. 26, no. 17, pp. 2142-2147, https://doi.org/10.1016/j.applthermaleng.2006.04.009

[28] R. Rayegan, Y. X. Tao, 2011. "A procedure to select working fluids for solar organic Rankine cycles (ORCs)," *Renewable Energy*, vol. 36, no. 2, pp. 659-670, https://doi.org/10.1016/j.renene.2010.07.010

[29] B. Saleh, G. Koglbauer, M. Wendland, J. Fischer, 2007. "Working fluids for low-temperature organic Rankine cycles," *Energy*, vol. 32, no. 7,

pp. 1210-1221, https://doi.org/10.1016/j.energy.2006.07.001

[30] A. M. Delgado-Torres, L. García-Rodríguez, 2010. "Analysis and optimization of the low-temperature solar organic Rankine cycle (ORC)," *Energy Conversion and Management,* vol. 51, no. 12, pp. 2846-2856, https://doi.org/10.1016/j.enconman.2010.06.022

[31] G. Kosmadakis, D. Manolakos, S. Kyritsis, G. Papadakis, 2009. "Economic assessment of a two-stage solar organic Rankine cycle for reverse osmosis desalination," *Renewable Energy*, vol. 34, no. 6, pp. 1579-1586, https://doi.org/10.1016/j.renene.2008.11.007

[32] H. Xi, M.-J. Li, C. Xu, Y.-L. He, 2013. "Parametric optimization of regenerative organic Rankine cycle (ORC) for low grade waste heat recovery using genetic algorithm," *Energy,* vol. 58, pp. 473-482, https://doi.org/10.1016/j.energy.2013.06.039

[33] S. Karellas, A. Schuster, A.-D. Leontaritis, 2012. "Influence of supercritical ORC parameters on plate heat exchanger design," *Applied Thermal Engineering,* vol. 33-34, pp. 70-76, https://doi.org/10.1016/j.applthermaleng.2011.09.013

[34] J. Zhang, W. Zhang, G. Hou, F. Fang, 2012. "Dynamic modeling and multivariable control of organic Rankine cycles in waste heat utilizing processes," *Computers & Mathematics with Applications*, vol. 64, no. 5, pp. 908-921, https://doi.org/10.1016/j.camwa.2012.01.054

[35] G. Hou, R. Sun, G. Hu, J. Zhang, 2011, "Supervisory predictive control of evaporator in organic Rankine cycle (ORC) system for waste heat recovery," in Proceedings of 2011 International *Conference on Advanced Mechatronic Systems*, Zhengzhou, China, pp. 306-311.

[36] H. Guo, Q. Wang, M. Jia, C. Zhang, 2018. "Multi-objective optimization of organic Rankine cycle system using multi-objective particle swarm optimization algorithm," *Energy Conversion and Management*, vol. 174, pp. 613-626,

[37] J. Peralez, P. Tona, M. Nadri, P. Dufour, A. Sciarretta, 2015. "Optimal control for an organic Rankine cycle on board a diesel-electric railcar," *Journal of Process Control*, vol. 33, pp. 1-13, https://doi.org/10.1016/j.jprocont.2015.03.009

[38] J. Larjola, 1995. "Electricity from industrial waste heat using high-speed organic Rankine cycle (ORC)," *International Journal of Production Economics,* vol. 41, no. 1-3, pp. 227-235, https://doi.org/10.1016/0925-5273(94)00098-0

[39] S. H. Kang, 2012. "Design and experimental study of ORC (organic Rankine cycle) and radial turbine using R245fa working fluid," *Energy*, vol. 41, no. 1, pp. 514-524, https://doi.org/10.1016/j.energy.2012.02.035

[40] E. H. Wang, H. G. Zhang, B. Y. Fan, M. G. Ouyang, Y. Zhao, Q. H. Mu, 2011. "Study of working fluid selection of organic Rankine cycle (ORC) for engine waste heat recovery," *Energy,* vol. 36, no. 5, pp. 3406-3418, https://doi.org/10.1016/j.energy.2011.03.041

[41] J. Bao, L. Zhao, 2013. "A review of working fluid and expander selections for organic Rankine cycle," *Renewable and Sustainable Energy Reviews,* vol. 24, pp. 325-342, https://doi.org/10.1016/j.rser.2013.03.040

[42] S. Quoilin, R. Aumann, A. Grill, A. Schuster, V. Lemort, H. Spliethoff, 2011. "Dynamic modeling and optimal control strategy of waste heat recovery organic Rankine cycles," *Applied Energy,* vol. 88, no. 6, pp. 2183-2190, https://doi.org/10.1016/j.apenergy.2011.01.015

[43] B. Dong, G. Xu, Y. Cai, H. Li, 2014. "Analysis of zeotropic mixtures used in high-temperature organic Rankine cycle," *Energy Conversion and Management,* vol. 84, pp. 253-260, https://doi.org/10.1016/j.enconman.2014.04.026

[44] H. Guo, Q. Wang, C. Zhang, J. Tian, 2019, "Nonlinear model predictive control of organic Rankine cycle for waste heat recovery," in 2019 IEEE 4th *International Conference on Advanced Robotics and Mechatronics (ICARM*), pp. 641-646.

[45] F. Campana, M. Bianchi, L. Branchini, A. De Pascale, A. Peretto, M. Baresi, A. Fermi, N. Rossetti, R. Vescovo, 2013. "ORC waste heat recovery in European energy intensive industries: Energy and GHG savings," *Energy Conversion and Management,* vol. 76, pp. 244-252, https://doi.org/10.1016/j.enconman.2013.07.041

[46] H. Chen, D. Y. Goswami, E. K. Stefanakos2010., "A review of thermodynamic cycles and working fluids for the conversion of low-grade heat," *Renewable and Sustainable Energy Reviews,* vol. 14, no. 9, pp. 3059-3067, https://doi.org/10.1016/j.rser.2010.07.006

[47] B. F. Tchanche, G. Lambrinos, A. Frangoudakis, G. Papadakis, 2011. "Low-grade heat conversion into power using organic Rankine cycles – A review of various applications," *Renewable and Sustainable Energy Reviews*, vol. 15, no. 8,

pp. 3963-3979, https://doi.org/10.1016/j.rser.2011.07.024

[48] V. Lemort, S. Quoilin, C. Cuevas, J. Lebrun, 2009. "Testing and modeling a scroll expander integrated into an organic Rankine cycle," *Applied Thermal Engineering*, vol. 29, no. 14-15, pp. 3094-3102, https://doi.org/10.1016/j.applthermaleng.2009.04.013

[49] E. Feru, F. Willems, B. de Jager, M. Steinbuch, 2014. "Modeling and control of a parallel waste heat recovery system for Euro-VI heavy-duty diesel engines," *Energies*, vol. 7, no. 10, pp. 6571-6592, https://doi.org/10.3390/en7106571

[50] C. Sprouse III, C. Depcik, 2013. "Review of organic Rankine cycles for internal combustion engine exhaust waste heat recovery," *Applied Thermal Engineering*, vol. 51, no. 1-2, pp. 711-722, https://doi.org/10.1016/j.applthermaleng.2012.10.017

[51] J. Bao, L. Zhao, W. Liu, 2013. "A review of working fluid and expander selections for organic Rankine cycle," *Renewable and Sustainable Energy Reviews*, vol. 24, pp. 325-342, https://doi.org/10.1016/j.rser.2013.03.040

[52] M. Badami, M. Mura, P. Campanile, F. Anzioso, 2008. "Design and performance evaluation of an innovative small scale combined cycle cogeneration system," *Energy*, vol. 33, no. 8, pp. 1264-1276, https://doi.org/10.1016/j.energy.2008.03.001

[53] S. Quoilin, R. Aumann, A. Grill, A. Schuster, V. Lemort, H. Spliethoff, 2011. "Dynamic modeling and optimal control strategy of waste heat recovery organic Rankine cycles," *Applied Energy*, vol. 88, no. 6, pp. 2183-2190, https://doi.org/10.1016/j.apenergy.2011.01.015

[54] F. Mertes, H. E. Ayed, P. Dufour, 2019. "Model-based control design of waste heat recovery organic Rankine cycle systems," *IFAC-PapersOnLine*, vol. 52, no. 5, pp. 424-429,

[55] J. Zhang, Y. Zhou, S. Gao, G. Hou, 2012. "Dynamic modeling and multivariable control of organic Rankine cycle in waste heat utilizing processes," *Computers & Mathematics with Applications*, vol. 64, no. 5, pp. 908-921, https://doi.org/10.1016/j.camwa.2012.01.054

[56] J. Peralez, P. Tona, M. Nadri, P. Dufour, A. Sciarretta, 2017. "Organic Rankine cycle for vehicles: Control design and experimental results," *IEEE Transactions on Control Systems Technology*, vol. 25, no. 3, pp. 952-965, https://doi.org/10.1109/tcst.2016.2574760

[57] X. D. Zhao, L. Bai, K. F. Yao, Z. R. Li, J. F. Wang, 2016, "Nonlinear model predictive control for organic Rankine cycle," in Proceedings of the 35th *Chinese Control Conference*, Chengdu, China, pp. 3769-3774.

[58] J. Zhang, Y. Zhou, R. Wang, J. Xu, F. Fang, 2014. "Modeling and constrained multivariable predictive control for ORC (Organic Rankine Cycle) based waste heat energy conversion systems," *Energy*, vol. 66, pp. 128-138, https://doi.org/10.1016/j.energy.2014.01.068

[59] H. Guo, Q. Wang, J. Tian, C. Zhang, 2017, "Real-time optimization and control of organic Rankine cycle systems using extremum seeking," in Proceedings of the 12th *IEEE Conference on Industrial Electronics and Applications*, Siem Reap, Cambodia, pp. 1628-1633.

[60] J. Peralez, P. Tona, A. Sciarretta, P. Dufour, M. Nadri, 2012, "Towards model-based control of a steam Rankine process for engine waste heat recovery," in 2012 *IEEE Vehicle Power and Propulsion Conference*, Seoul, South Korea, pp. 289-294. https://doi.org/10.1109/vppc.2012.6422718

[61] G. Hou, R. Sun, G. Hu, J. Zhang, 2011, "Supervisory predictive control of evaporator in organic Rankine cycle (ORC) system for waste heat recovery," in Proceedings of 2011 *International Conference on Advanced Mechatronic Systems*, Zhengzhou, China, 2011, pp. 306-311. https://doi.org/10.2514/6.2022-1406.vid

[62] S. Quoilin, V. Lemort, J. Lebrun, 2010. "Experimental study and modeling of an organic Rankine cycle using scroll expander," *Applied Energy*, vol. 87, no. 4, pp. 1260-1268, https://doi.org/10.1016/j.apenergy.2009.06.026

[63] S. Lecompte, H. Huisseune, M. van den Broek, B. Vanslambrouck, M. De Paepe, 2015. "Review of organic Rankine cycle (ORC) systems for waste heat recovery," *Renewable and Sustainable Energy Reviews*, vol. 47, pp. 448-461,

[64] J. M. Luján, J. R. Serrano, V. Dolz, J. Sánchez, 2012. "Model of the expansion process for R245fa in an organic Rankine cycle (ORC)," *Applied Thermal Engineering*, vol. 40, pp. 248-257, https://doi.org/10.1016/j.applthermaleng.2012.02.020

[65] M. O. Bamgbopa, E. Uzgoren, 2013. "Numerical analysis of an organic Rankine cycle under steady and variable heat input," *Applied Energy*, vol. 107, pp. 219-228, https://doi.org/10.1016/j.apenergy.2013.02.040

[66] S. Quoilin, M. Orosz, H. Hemond, V. Lemort, 2011. "Performance and design optimization of a low-cost solar organic Rankine cycle for remote

power generation," *Solar Energy*, vol. 85, no. 5, pp. 955-966,
https://doi.org/10.1016/j.solener.2011.02.010

[67] J. Zhang, Y. Zhou, Y. Li, G. Hou, F. Fang, 2013. "Generalized predictive control applied in waste heat recovery power plants," *Applied Energy*, vol. 102, pp. 320-326, https://doi.org/10.1016/j.apenergy.2012.07.038

[68] Zhang, J., Zhou, Y., Wang, R., Xu, J., & Fang, F. (2019). Modeling and constrained multivariable predictive control for ORC (Organic Rankine Cycle) based waste heat energy conversion systems. *Energy*, 143, 1030-1045. https://doi.org/10.1016/j.energy.2014.01.068

[69] Liu, L., Zhu, T., & Ma, J. (2020). Experimental investigation on the dynamic behavior of organic Rankine cycle system driven by engine exhaust heat. *Applied Thermal Engineering*, 168, 114854.

[70] Hernandez, A., Desideri, A., Ionescu, C., & De Keyser, R. (2021). Increasing the efficiency of Organic Rankine Cycle Technology by means of Multivariable Predictive Control. *Applied Energy*, 282, 116107.
https://doi.org/10.3182/20140824-6-za-1003.01796

[71] Kim, J. S., Kim, D. Y., & Kim, Y. T. (2022). Data-driven nonlinear model predictive control for organic Rankine cycle systems using deep learning. *Energy*, 239, 122173.